（倫理面への配慮）

全国調査における患者の個人情報に関しては、施設外へ出さないように匿名化して分析を行なう。医療情報の利用に関しては、匿名化した利用に関して十分な説明と同意を得る様にし、必要に応じて施設の倫理審査委員会の承認を受ける様にする。日本小児外科学会認定施設における調査に関しては、同学会学術委員会に申請し、審査のうえ承認を得た。

診断基準、重症度評価、診療ガイドラインの策定に関しては、研究施設の倫理審査申請対象には該当しない。

C．研究結果

1）診断基準案

これまでの全国調査のデータでは、本研究班でいう有症状性の肝血管腫に該当する症例の診断時年齢は0～5ヶ月（中央値１ヶ月）で、いづれも極めて早い月齢で診断されていた。中には出生前診断されている症例も含まれた。また、肝内病変は文献的に指摘される様な瀰漫性病変のほか、単発性病変においても死亡例があることが分かった。本邦における肝内単発性病変で死亡した症例のうち最も径の小さな病変は診断時の径80mmであった。多発病変で有症状の症例を見ると、肝内病変の数は2～10個となっており、最低２病変でも症状を呈しうることが分かった。

これらの調査データに基づいて診断の手引きとして診断基準案を策定した。即ち、本研究班でいう「乳児巨大血管腫」とは生後１歳未満の乳児、新生児で有症状性の肝内血管性病変を有するものと規定し、病変については単発で巨大なものと、肝を４分割ひたうち２つ以上の区域に病変を持つものと規定した。さらに巨大病変の定義として、径80mmで死亡例があったことから、１歳未満の計測で25%の安全率をおいて径60mm以上のものと規定した。さらに肝血管腫に現れた臨床症状、付随症状を診断の手引きに含めた。また鑑別診断として、に肝芽腫などの原発性肝悪性腫瘍を削除する様に規定した。（添付資料１）

2）重症度分類

重症度分類案は生命の危険が差し迫っている「重症」、何らかの生命維持に関わる症状があり放置すれば生命の危険がある「中等症」、それ以外の「軽症」と３段階に分類した。死亡例の検討では治療前の血小板数の最高値は13,300/mm3であった。死亡例では全て治療に対して血小板数の増加は見られていなかった。またプロトロンビン時間をみると死亡例で最も延長していなかった症例のプロトロンビン時間は19.6秒で、死亡例では治療による凝固障害の改善は見られていなかった。これらのでーたに基づいて、生命の危険が迫っている症例は血小板数が10,000/mm3未満、プロトロンビン時間が20秒以上に延長、あるいは治療に反応した血小板数減少や凝固障害の改善がみられないものとした。（添付資料２）

3）クリニカル・クエッションの検討

「乳児巨大肝血管腫」の診療ガイドライン策定にあたり、クリニカル・クエッションを「診断」、「治療」、「長期予後」の３分野に大別することとした。「長期予後」の項を設けたのは、やはり全国調査のなかで、乳児期の治療に反応して肝内病変

が一度は退縮傾向を見せ、呼吸循環障害や血液凝固障害の改善を見た後に、幼児期に門脈大循環シャント血流の増大から肝不全徴候が顕著になった症例が発見されたためである。MINDS2014年版の手引きに従って、PICO（Patients, Iinterventions/Compari-sons, Outcomes）をそれぞれに規定した。今後のシステマティック・レビューの文献検索作業に向けて、Interventions/Comparisonsを細かく上げ、Outcomeは呼吸循環障害、血液凝固障害の改善の有無とした。（添付資料３）

D．考察

本年度は「乳児巨大肝血管腫」の診療ガイドライン策定の基盤として、昨期までの研究班で集積した臨床情報、構築されたデータベースの見直しを行い、それを基にして「乳児巨大肝血管腫」の疾患概念の既定を行った。概念の既定にあたっての詳細は結果の項に述べた。これにより、これまで曖昧であった乳幼児の難治性の肝血管腫に、客観的な診断基準が既定された。

重症度評価は生命の危機を軸に、死亡例と生存例の比較からハイリスク因子を規定した。

「乳児巨大肝血管腫」に該当するような症例の頻度は、全国で年間に5-10例程度と推定されている。こうした症例の存在は古くより知られていたものの、４次にわたる過去の調査では、実際の頻度は考えられていた以上に稀少であることが分かった。こうした稀少疾患のガイドライン策定に、MINDSの手引きのような手法が有用か否かは議論のあるところである。稀少疾患の診療ガイドラインには専門家の意見の方がより重きを占める可能性もある。全国的な調査研究も、一般的にはRCTに比較するとエビデンスレベルが低く考えられるが、疾患概念が本邦と例えばボストングループのChristison-Lagayらとも異なっているため、本邦のガイドラインでは他グループの調査文献は有用性が高くないと言わざるを得ない。本疾患のガイドライン策定には、当初からこうした問題が付随しており、今後、これを認識して作業を進めて行く必要があるものと思われる。

今年度は疾患概念の既定からクリニカル・クエッションの検討まで進められたが、次年度以降に、スコープの完成、クリニカル・クエッションの確定、そしてシステマティック・レビューへと作業を進めて行く予定である。

E．結論

１）これまでの厚生労働省難治性疾患克服研究事業における調査結果を見直して、乳児巨大肝血管腫の概念を１歳未満の単発性・多発性の肝内血管性病変をもつ有症状例と規定し、診断基準案および重症度分類案を策定した。

２）乳児巨大肝血管腫に対する診療ガイドライン策定の手掛かりとして、クリニカル・クエッションとそれに関するPICO事項がまとめられた。

F．研究発表

１．論文発表

1) Kuroda,T, Hoshino, K, Nosaka S, et al: Critical hepatic hemangioma in infants: recent nationwide survey in Japan. Pediatr Int 2014; 56:304-308

2) 黒田達夫：新生児の難治性良性腫瘍の現状と展望　難治性肝血管腫　周産期学シンポジウム　2014；32：39− 42

3) 黒田達夫、星野健、藤野明浩、他：肝血管腫　周産期医学　2014；44：1369-1372

２．学会発表
なし

G．知的所有権の出願・登録状況（予定を含む）

１．特許取得
該当なし

２．実用新案登録
該当なし

３．その他

（添付資料１）

【診断基準案】

新生児・乳児難治性肝血管腫
診断の手引き

生後1歳未満より肝実質内を占拠する有症状性の血管性病変があり、以下の2項目の双方を満たす。

1) 生後1歳未満の画像所見で、肝内に単発で径60mm以上、または右外側、右内側、左内側、左外側の4区域のうち2区域以上に及ぶ多発の血管性病変を有する。（画像診断）
2) 以下にあげるうち一つ以上の症状を呈するもの：
   呼吸異常、循環障害、凝固異常、血小板減少、
   腎不全、肝腫大、肝機能障害、甲状腺機能低下、
   体重増加不良

付記　本症を疑う参考所見
　　高ガラクトース血症、高アンモニア血症、皮膚血管腫

鑑別診断　肝芽腫など肝原発の悪性腫瘍は除く

（添付資料２）

【重症度分類案】

新生児・乳児難治性肝血管腫
重症度分類案

・ 重症：生命の危険が差し迫っているもの
　凝固異常（PT20秒以上）
　血小板減少（血小板数<10万/mm3）
　Steroid投与に対してPT活性、血小板数の低下が
　　改善しないもの

・中等症：放置すれば生命の危険があるもの
　下に上げるうち一つ以上の徴候がみられるもの
　　心機能低下
　　呼吸障害
　　肝不全徴候

・軽症：上記以外

（添付資料３）

【ガイドライン　クリニカルクエッション案】

【診断】

「乳幼児肝巨大血管腫」について：疫学、診断基準など概要の解説

CQ１．至急治療を要する重症例をどのように診断するか

【治療】

CQ２．急性期の呼吸循環障害に有効な治療は何か

P：乳幼児肝巨大血管腫（呼吸循環障害のある症例）

I/C：ステロイド投与例・非投与例
プロプラノロール投与例・非投与例
抗がん剤投与例・非投与例
IVR 塞栓療法施行例・非施行例
放射線療法施行例・非施行例
外科手術例。非手術例

O：呼吸循環障害の改善

CQ３．急性期の血液凝固障害に有効な治療は何か

P：乳幼児肝巨大血管腫（血液凝固障害のある症例）

I/C：ステロイド投与例・非投与例
プロプラノロール投与例・非投与例
抗 DIC 治療施行例・非施行例
抗がん剤投与例・非投与例
IVR 塞栓療法施行例・非施行例
放射線療法施行例・非施行例
外科手術例・非手術例

O：血液凝固障害の改善

【長期予後】

CQ４．慢性期の肝不全に肝移植は有用か

P：乳幼児肝巨大血管腫で年長児に肝障害を呈した症例

I/C：肝移植施行例・非施行例

O：長期生存の有無

厚生労働科学研究　難治性疾患等政策研究事業(難治性疾患克政策究事業)
「難治性血管腫・血管奇形・リンパ管種・リンパ管種症および関連疾患についての調査研究班」
平成26年度　研究報告書

診療報酬記録からみた末梢性動静脈奇形、クリッペル・トレノネー症候群結果、クリッペル・トレノーネイ・ウェーバ症候群の全国推定患者数の算出

研究分担者　　田中 純子
(広島大学　大学院医歯薬保健学研究院　疫学・疾病制御学　教授)

研究協力者　　大久 真幸
(広島大学　大学院医歯薬保健学研究院　疫学・疾病制御学　助教)

研究要旨

健康保険組合は全国約1,500あり、その対象者数は約3,000万人である。そのうち、20の健康保険組合に属する本人および家族の全診療報酬記録(レセプト)データを解析対象として血管腫・血管奇形関連患者数の把握を試みた。観察期間と対象数は2009年(3,743,902レセプト、818,359人)、2010年(5,451,612レセプト、1,176,754人)、2011年(6,056,650レセプト、1,251,949人)(対象年齢:0歳~74歳)である。

標準病名が末梢性同静脈奇形、クリッペル・トレノネー症候群、クリッペル・トレノーネイ・ウェーバ症候群であるレセプトを抽出し、65歳以上・疑診例のレセプトを除外した。

個人識別ID別、時系列別に詳細に検討し、性別・年齢別に期間有病率を算出した。算出した有病率と日本人口を元に全国推定実患者数を算出した。その結果、2009.1~2009.12の1年期間有病率をもとに算出した64歳以下の末梢性同静脈奇形の全国推定実患者数は209人(95%CI:39-6,620人)、クリッペル・トレノネー症候群は0人(95%CI:0-6,627人)、クリッペル・トレノーネイ・ウェーバ症候群422人(95%CI:0-5,978人)であった。今回の結果は有病率が非常に小さい事から95%信頼区間が大きくなったため、更なる検討が必要である。

A 研究目的

患者数の把握が困難な希少疾患である難治性血管腫・血管奇形のうち、末梢性同静脈奇形、クリッペル・トレノネー症候群、クリッペル・トレノーネイ・ウェーバ症候群の患者数を、健康保険組合に加入している本人および家族の全診療報酬記録（以下レセプト）のデータから推計することを試みた。

B 研究方法

1) 解析対象

健康保険組合は全国約 1,500 あり、その対象者数は約 3,000 万人である。そのうち、20 の健康保険組合に属する本人および家族の全診療報酬記録を解析対象とした。

観察期間と対象数は 2009 年（3,743,902 レセプト、818,359 人）、2010 年（5,451,612 レセプト、1,176,754 人）、2011 年（6,056,650 レセプト、1,251,949 人）（対象年齢：0 歳～74 歳）である。

解析対象の 2011 における年齢分布を 2011 における日本全体の年齢分布と比較すると、高齢者の割合が低いことがわかる（図 1）。

2)解析方法

上記対象レセプトの、標準病名が末梢性同静脈奇形、クリッペル・トレノネー症候群、クリッペル・トレノーネイ・ウェーバ症候群であるものを抽出した。抽出したレセプトを個人識別 ID・診療年月でソートし、性・年齢階級別・疾患別に集計して 1 年期間有病率を算出した。算出した 1 年期間有病率と人口から全国推定実患者数を算出した。また、65 歳以上の対象集団が少ないため 64 歳以下の集計を行った。

C 結果

算出した 1 年期間有病率を元に日本における 64 歳以下の全国推定実患者数及び

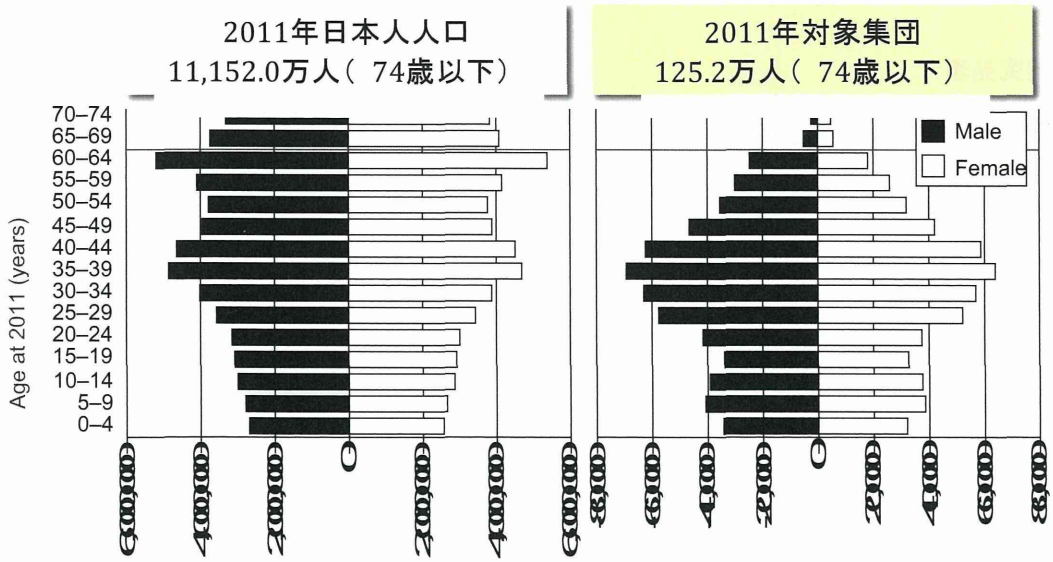

図 1 2011 年 10 月時の人口ピラミッド（左）2011 年における対象者の数(右)

表 1 1 年期間有病率を基に算出した疾患別全国推定患者数

	2009年	2010年	2011年
末梢性動静脈奇形	209 (39-6,620)	277 (25-6,991)	696 (56-5,702)
クリッペル・トレノネー症候群結果	0 (0-6,627)	108 (0-7,046)	0 (0-6,323)
クリッペル・トレノーネイ・ウェーバ症候群結果	422 (0-5,978)	748 (60-6,547)	626 (70-5,771)

全国推定延べ患者数を表 1 に示す。全国推定実患者数は 3 年間を通じて大きな変動は認められなかった。2009 年における 64 歳以下の末梢性同静脈奇形の全国推定実患者数は 209 人(95%CI: 39–6,620 人)、クリッペル・トレノネー症候群は 0 人（95%CI: 0-6,627 人）、クリッペル・トレノーネイ・ウェーバ症候群 422 人（95%CI: 0-5,978 人）であった。

D. 結論と考察

今回、比較的規模が大きく全国に支店を持つ事業所が加入している健康保険組合の本人および家族の 2009–2011 年における全レセプトデータをもとにした患者数の推定を試みた。

今回の結果は、有病率が非常に小さくなった事から 95%信頼区間が大きくなったため、更なる検討が必要である。

E 研究発表

該当なし

F 健康危険情報

該当なし

G 知的財産権の出現・登録状況

該当なし

III　研究成果の刊行に関する一覧表

研究成果の刊行に関する一覧表

書籍

著者氏名	論文タイトル名	書籍全体の編集者名	書籍名	出版社名	出版地	出版年	ページ
Akita S, Houbara S and Akatsuka M.	Imaging, vascular assessment: Extension in depth and vascular anomalies.	Teot L, Meaume S, Del Mamol V, Akita S, Ennis WI.	Skin Necrosis	Springer-Verlag	Heidelberg	2014	19-24

雑誌

発表者氏名	論文タイトル名	発表誌名	巻号	ページ	出版年
Hata Y, Osuga K, Uehara S, Yano K, Kikuchi M, Tomita K, Matsuda K, Kubo T, Fujiwara T, Hosokawa K.	Topological Analysis for Arteriovenous Malformations via Computed Tomography Angiography: Part 2: Practical Application.	Plast Reconstr Surg Glob Open	2	e207	2014
Hata Y, Osuga K, Kubo T, Matsuda K, Tomita K, Kikuchi M, Fujiwara T, Yano K, Hosokawa K.	Topological Analysis for Arteriovenous Malformations via Computed Tomography Angiography: Part 1: Mathematical Concepts.	Plast Reconstr Surg Glob Open	2	e205	2014
Nakamura M, Osuga K, Maeda N, Higashihara H, Hamada K, Hashimoto N, Uehara S, Tomiyama N.	Percutaneous sclerotherapy for venous malformations in the extremities: clinical outcomes and predictors of patient satisfaction.	SpringerPlus	3	609	2014
Osuga K, Kishimoto K, Tanaka K, Nakamura M, Ono Y, Maeda N, Higashihara H, Nakazawa T, Tomiyama N	Initial experience with use of hydrogel microcoils in embolization of pulmonary arteriovenous malformations	SpringerPlus	3	609	2014
Akita S, Houbara S and Hirano A.	Management of vascular malformations.	Plast Reconstr Surg Glob Open	2	e128	2014
Houbara S, Akita S, Yoshimoto H and Hirano A	Vascular malformations that were diagnosed as or accompanied by malignant tumors.	Dermatol Surg	40	1225-1232	2014

発表者氏名	論文タイトル名	発表誌名	巻号	ページ	出版年
Arita Y, Nakaoka Y, Matsunaga T, Kidoya H, Yamamizu K, Arima Y, Kataoka-Hashimoto T, Ikeoka K, Yasui T, Masaki T, Yamamoto K, Higuchi K, Park JS, Shirai M, Nishiyama K, Yamagishi H, Otsu K, Kurihara H, Minami T, Yamauchi-Takihara K, Koh GY, Mochizuki N, Takakura N, Sakata Y, Yamashita JK, Komuro I.	Myocardium-derived angiopoietin-1 is essential for coronary vein formation in the developing heart.	Nat Commun	29	4552	2014
Ishikura K, Misu H, Kumazaki M, Takayama H, Matsuzawa-Nagata N, Tajima N, Chikamoto K, Lan F, Ando H, Ota T, Sakurai M, Takeshita Y, Kato K, Fujimura A, Miyamoto K, Saito Y, Kameo S, Okamoto Y, Takuwa Y, Takahashi K, Kidoya H, Takakura N, Kaneko S, Takamura T.	Selenoprotein P as a diabetes-associated hepatokine that impairs angiogenesis by inducing VEGF resistance in vascular endothelial cells.	Diabetologia	57	1968-76	2014
Ohnishi K, Tagami M, Morii E, Azumi A.	Topical Treatment for Orbital Capillary Hemangioma in an Adult Using a ß-Blocker Solution.	Case Rep Ophthalmol	20	60-65	2014
Kuroda,T, Hoshino, K, Nosaka S, et al	Critical hepatic hemangioma in infants: recent nationwide survey in Japan.	Pediatr Int	56	304-308	2014
藤野明浩, 高橋信博, 石濱秀雄, 藤村匠, 加藤源俊, 富田紘史, 渕本康史, 星野健, 黒田達夫	気道周囲を取り巻く頸部・縦隔リンパ管腫切除	小児外科	46	105-110	2014
藤野明浩, 森定徹, 梅澤明弘, 黒田達夫	ヒトリンパ管腫モデル動物の作成	小児外科	46	635-638	2014
藤野明浩, 上野滋, 岩中督, 木下義晶, 小関道夫, 森川康英, 黒田達夫	リンパ管腫	小児外科	46	1181-1186	2014
田倉智之	米国のRBRVsにみる医師技術料評価の考え方	日本内科学会誌	103	15-23	2014
田倉智之	産業政策としての先端医療	病院	73	528-533	2014

発表者氏名	論文タイトル名	発表誌名	巻号	ページ	出版年
黒田達夫	新生児の難治性良性腫瘍の現状と展望　難治性肝血管腫	周産期学シンポジウム	32	39-42	2014
黒田達夫、星野健、藤野明浩、他	【胎児・新生児の肝・胆道疾患】外科疾患　肝血管腫	周産期医学	44	1369-1372	2014
三村秀文、芝本健太郎、宗田由子、児島克英、松井裕輔、藤原寛康、平木隆夫、郷原英夫、金澤　右	軟部動静脈奇形の塞栓術	臨床画像	30	516-523	2014
三村秀文、芝本健太郎、宗田由子、児島克英、松井裕輔、藤原寛康、平木隆夫、郷原英夫、金澤　右	静脈奇形の硬化療法	臨床放射線	59	524-532	2014

Ⅳ　研究成果の刊行物・別冊

Topological Analysis for Arteriovenous Malformations via Computed Tomography Angiography: Part 1: Mathematical Concepts

Yuki Hata, MD*
Keigo Osuga, MD, PhD†
Tateki Kubo, MD, PhD*
Ken Matsuda, MD, PhD*
Koichi Tomita, MD, PhD*
Mamoru Kikuchi, MD, PhD*
Takashi Fujiwara, MD*
Kenji Yano, MD, PhD*
Ko Hosokawa, MD, PhD*

Background: Evaluating the progression of soft-tissue arteriovenous malformation (AVMs) is still problematic. To establish a quantitative method, we took a morphological approach.
Methods: Normal blood vessels in early-phase 3D-computed tomography angiography images are theoretically expected to be tree-like structures without loops, whereas AVM blood vessels are expected to be mesh-like structures with loops. Simplified to the utmost limit, these vascular structures can be symbolized with wire-frame models composed of nodes and connecting edges, in which making an extra loop always needs one more of edges than of nodes.
Results: Total amount of abnormal vascular structures is estimated from a simple equation: Number of vascular loops = 1 − ([Number of nodes] − [Number of edges]).
Conclusion: Abnormalities of AVM vascular structures can be mathematically quantified using computed tomography angiography images. *(Plast Reconstr Surg Glob Open 2014;2:e205; doi: 10.1097/GOX.0000000000000163; Published online 28 August 2014.)*

Soft-tissue arteriovenous malformations (AVMs) progress asymptomatically or recur indistinguishably from normal blood vessels. Despite that, understanding of their progression usually relies on approximate staging according to symptoms[1] or qualitative visual assessment of imaging examinations. Against this dilemma, numerous attempts have been made to establish quantitative evaluation methods.

*From the *Department of Plastic Surgery, Osaka University Graduate School of Medicine, Osaka, Japan; and †Department of Diagnostic and Interventional Radiology, Osaka University Graduate School of Medicine, Osaka, Japan.*
Received for publication December 27, 2013; accepted June 25, 2014.
Copyright © 2014 The Authors. Published by Lippincott Williams & Wilkins on behalf of The American Society of Plastic Surgeons. PRS Global Open is a publication of the American Society of Plastic Surgeons. This is an open-access article distributed under the terms of the Creative Commons Attribution-NonCommercial-NoDerivatives 3.0 License, where it is permissible to download and share the work provided it is properly cited. The work cannot be changed in any way or used commercially.
DOI: 10.1097/GOX.0000000000000163

From a functional viewpoint, evaluation of total shunt blood flow using transarterial lung perfusion scans[2–4] and measurement of blood pool volume with whole-body blood pool scans by Lee et al[2,4,5] are the most quantitative methods. However, these methods based on nuclear medicine are problematic for their invasion and limited site of application.

From a morphometric viewpoint, Kaji et al[6] used magnetic resonance imaging and World Health Organization Response Criteria (product of lesion major and minor axes in cross-section). However, it is difficult to apply it to vascular malformations, which are irregular in shape with indistinct borders, easily expanding and collapsing.

Considering these unmet needs, we searched for another approach to meet the anatomical nature of AVMs and set the first research objective to establish a morphological solution to quantify abnormalities of AVM vascular structures.

Disclosure: *The authors have no financial interest to declare in relation to the content of this article. The Article Processing Charge was paid for by the authors.*

Copyright © 2014 The Authors. Published by Lippincott Williams & Wilkins on behalf of The American Society of Plastic Surgeons.
PRS Global Open is a publication of the American Society of Plastic Surgeons.

METHODS

We anticipated utilization of computed tomography angiography (CTA) results for retrospective evaluation because it is a widespread, less-invasive method of testing AVMs. Moreover, because of their relatively higher contrast, obtaining clear and stable vascular segmentation[7] is easier than Magnetic Resonance Angiography (MRA).[8–10]

We also applied 2 mathematical theories, namely topology and graph theory, to quantify abnormalities of vascular structures.

Simplification via Topological Homeomorphism

Topology is a relatively new field of geometry that focuses on the continuity of regions. For example, as both a coffee cup and a donut share the feature of having only one hole (loop), they are considered homeomorphic with deformation.

Viewed through homeomorphic simplification, the number of loops in an early-phase 3D-CTA image of a normal blood vessel is theoretically expected to be close to zero except for physiological vascular rings, such as at the base of the brain. It is because arteries branch off repeatedly from the aorta and are not rendered with the standard CT resolution after they become arterioles (approximate diameter, 0.1–0.2 mm) (Fig. 1).

Meanwhile, the presence of a described arteriovenous shunt is depicted on early-phase 3D-CTA images as a series of pathways from the feeding artery to the drainage vein. Furthermore, the more abnormal intervascular shortcut appears, the more external loop develops or an existing loop divides.

Quantification of Connectivity with Graph Theory

The appropriate method for loop measurement is graph theory, which is being utilized for engineering problems such as electric circuits and train routes.

If one focuses only on connectivity and dispenses with all other data such as thickness and length, the vascular structure can ultimately be symbolized into a "graph" composed of nodes and edges joining them. The number of loops in the graph can be calculated by a simple calculation using the number of nodes and edges. The principle can be verified and understood by using our "spaghetti and marshmallows vascular model." This model can be actually manipulated according to only one rule that a marshmallow (node) must be positioned on the tip of each piece of spaghetti (edge).

When a model only diverges and expands repeatedly like the branches or roots of a tree, the total number of nodes keeps one more than edges. It is because one node is needed for every new edge when branches are added or divided (Fig. 2A).

However, when nodes and edges are added to increase the number of loops, the number of edges will only increase by one extra piece each time. This is because even if a new loop is added or the existing loop is divided, one more edge is needed compared with nodes (Fig. 2B).

RESULTS

Aforementioned mathematical concepts lead to a principle that abnormal connectivities within an AVM lesion can be quantified with the increase of difference between the number of nodes and edges comprising its wire-framed network model. This principle is depicted by the following simple equation:

$$\text{Number of vascular loops} = 1-\left(\left[\text{Number of nodes}\right]-\left[\text{Number of edges}\right]\right).$$

DISCUSSION

Fundamental Limitation

In clinical applications, there is an inevitable limitation that the number of vascular loops calculated from CTA images is not necessarily the histological amount of arteriovenous shunts within the actual lesion but "describable" shunts to the utmost. However, it is rather the common fundamental limitation for all imaging examinations.

Resolution Constancy

There are 2 important points regarding this technique. The first is that image resolution affects the detection of continuity. For example, the relationship of a blood vessel with its accompanying vessel 0.3 mm away can be sometimes correctly displayed on an image with 0.27 × 0.27 mm pixel size but invari-

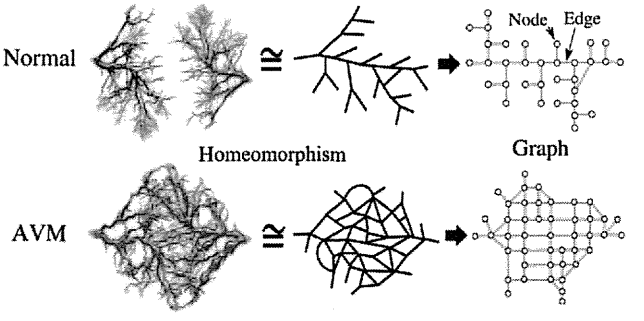

Fig. 1. Conceptual workflow images of homeomorphic simplification and symbolization of vascular structures. AVM graphs are assumed to be more perforated than normal blood vessel graphs.

Copyright © 2014 The Authors. Published by Lippincott Williams & Wilkins on behalf of The American Society of Plastic Surgeons.
PRS Global Open is a publication of the American Society of Plastic Surgeons.

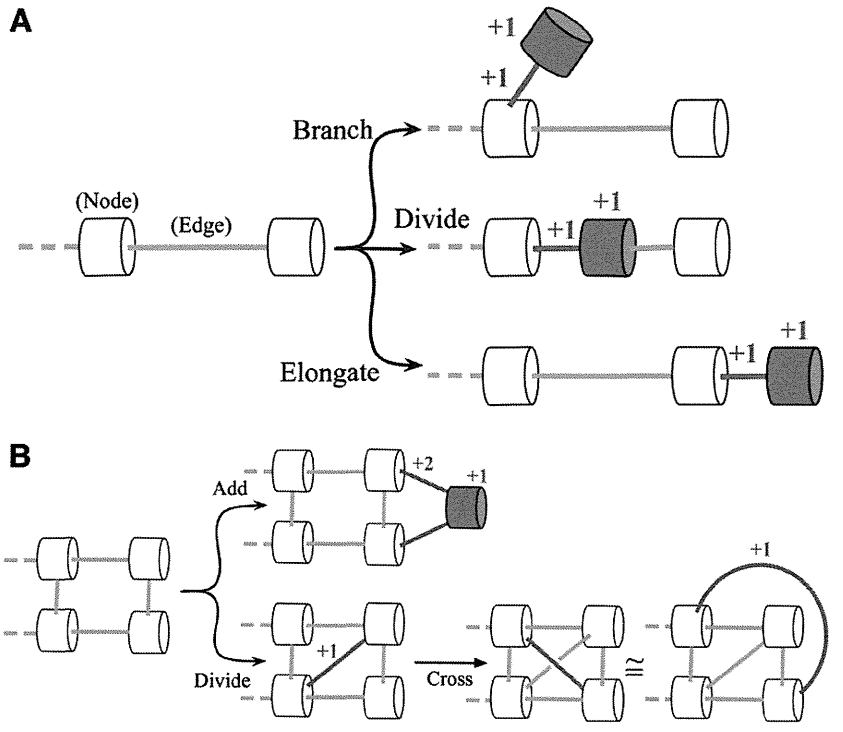

Fig. 2. Verification of graph theory with "spaghetti and marshmallows vascular models." A, Tree-type growth: when a model only diverges and expands repeatedly like the branches or roots of a tree, the gap of nodes and edges never changes. B, Mesh-type growth: when nodes and edges are added to increase the number of loops from that of the original model, the number of edges will only increase by one extra piece each time. This principle holds true even in 3-dimensionally (3D) complex angioarchitecture because an internal 3D crossing is topologically homeomorphic with an external handle.

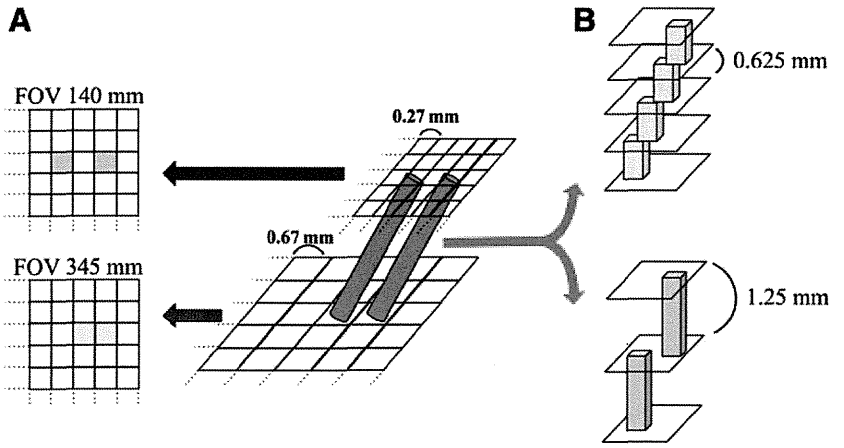

Fig. 3. The influence of imaging conditions. A, When a computed tomography section is provided as a 512×512 pixel image, the relationship of a blood vessel with its accompanying vessel 0.3 mm away can be sometimes correctly displayed on a 140-mm field-of-view (FOV) (pixel size, 0.27×0.27 mm) image of the peripheral extremities, while the same 2 vessels can invariably be displayed as being connected on a 345-mm FOV (pixel size, 0.67×0.67 mm) image of the trunk. B, Vessels rendered as continuous on images with a section thickness of 0.625 mm might appear to be not continuous on images with section thicknesses of 1.25 mm.

Copyright © 2014 The Authors. Published by Lippincott Williams & Wilkins on behalf of The American Society of Plastic Surgeons.
PRS Global Open is a publication of the American Society of Plastic Surgeons.

ably be displayed as being connected on an image with 0.67×0.67 mm pixel size (Fig. 3A).

Conversely, oblique vessels rendered as continuous on images with a section thickness of 0.625 mm might appear to be not continuous on images with section thicknesses of 1.25 mm (Fig. 3B).

Field of view and section thickness must be identical to compare test results obtained at different times from a same patient. In addition, even in patients with a common lesion site, the closer the test field of view and section thickness are, the more meaningful the comparison is.

Region of Interest Constancy

The second point is that one cannot be sure that region of interest has been uniformly maintained through the series of results especially when efficient procedure causes drastic change to the lesion hemodynamics. Region of interest must be identical before and after treatment, which is possible if clear, fixed points such as the junctions of well-known blood vessels or feeding arteries are used as reference points.

CONCLUSIONS

It seems that the mathematical concepts of topology and graph theory can be used to quantify abnormalities of AVM vascular structures from CTA images. Careful assessment of validity through practical application is necessary for this novel concept.[11]

Yuki Hata, MD
Department of Plastic Surgery
Osaka University Graduate
School of Medicine, Osaka, Japan
E-mail: yukihata@gmail.com

REFERENCES

1. Kohout MP, Hansen M, Pribaz JJ, et al. Arteriovenous malformations of the head and neck: natural history and management. *Plast Reconstr Surg.* 1998;102:643–654.
2. Lee BB, Do YS, Yakes W, et al. Management of arteriovenous malformations: a multidisciplinary approach. *J Vasc Surg.* 2004;39:590–600.
3. Vaišnytė B, Vajauskas D, Palionis D, et al. Diagnostic methods, treatment modalities, and follow-up of extracranial arteriovenous malformations. *Medicina (Kaunas).* 2012;48:388–398.
4. Lee BB, Mattassi R, Kim YW, et al. Advanced management of arteriovenous shunting malformation with transarterial lung perfusion scintigraphy for follow-up assessment. *Int Angiol.* 2005;24:173–184.
5. Lee BB, Mattassi R, Kim BT, et al. Contemporary diagnosis and management of venous and arterio-venous shunting malformation by whole body blood pool scintigraphy. *Int Angiol.* 2004;23:355–367.
6. Kaji N, Kurita M, Ozaki M, et al. Experience of sclerotherapy and embolosclerotherapy using ethanolamine oleate for vascular malformations of the head and neck. *Scand J Plast Reconstr Surg Hand Surg.* 2009;43:126–136.
7. Moore EA, Grieve JP, Jäger HR. Robust processing of intracranial CT angiograms for 3D volume rendering. *Eur Radiol.* 2001;11:137–141.
8. Suazo L, Foerster B, Fermin R, et al. Measurement of blood flow in arteriovenous malformations before and after embolization using arterial spin labeling. *Interv Neuroradiol.* 2012;18:42–48.
9. Albert CS, Chung JAN. Statistical 3d vessel segmentation using a rician distribution. Available at: http://citeseerx.ist.psu.edu/viewdoc/summary?doi=10.1.1.75.2885. Accessed June 27, 2013.
10. Bullitt E, Aylward S, Bernard EJ, et al. Computer-assisted visualization of arteriovenous malformations on the home personal computer. *Neurosurgery* 2001;48:576–582; discussion 582–583.
11. Hata Y, Osuga K, Uehara S, et al. Topological analysis for arteriovenous malformations via computed tomography angiography: part 2: practical application. *Plast Reconstr Surg Glob Open* 2014. doi: 10.1097/GOX.0000000000000151.

Copyright © 2014 The Authors. Published by Lippincott Williams & Wilkins on behalf of The American Society of Plastic Surgeons.
PRS Global Open is a publication of the American Society of Plastic Surgeons.

OPEN

ORIGINAL ARTICLE
Pediatric/Craniofacial

Topological Analysis for Arteriovenous Malformations via Computed Tomography Angiography: Part 2: Practical Application

Yuki Hata, MD*
Keigo Osuga, MD, PhD†
Shuichiro Uehara, MD, PhD‡
Kenji Yano, MD, PhD*
Mamoru Kikuchi, MD, PhD*
Koichi Tomita, MD, PhD*
Ken Matsuda, MD, PhD*
Tateki Kubo, MD, PhD*
Takashi Fujiwara, MD*
Ko Hosokawa, MD, PhD*

Background: In a previous study, the authors outlined a technique for calculating the number of abnormal vascular loop structures described in 3-dimensional computed tomography angiography. To be developed into a quantitative evaluation method for soft-tissue arteriovenous malformations (AVMs), the concept needs assessment of validity.
Methods: Computed tomography angiography results of 19 soft-tissue AVMs and 18 control abdominal vessels are utilized. Enhanced vascular lumen regions over 120 HU were extracted by a region growing method and skeletonized into wire frame graph models. The number of vascular loop structures in graphs is calculated as 1 − [Number of nodes] + [Number of edges], and results are compared between AVM/control groups, pre-/postprogression, and pre-/posttreatment.
Results: Average vascular lumen capacity of AVMs was 57.5 ml/lesion, and average number of vascular loops was 548 loops/lesion. Loop density of AVMs (weighted average, 9.5 loops/ml) exhibited statistically significant ($P < 0.001$) greater value than normal abdominal blood vessels (weighted average, 1.3 loops/ml). In all 4 cases without treatment, number of loops and loop density both increased. Particularly, number of loops increased greatly by 2 times or more in 3 cases. In all 7 cases with treatment, number of loops and vascular lumen capacity significantly ($P = 0.0156$) decreased. Particularly, number of loops showed clearer decrease in cases with entire lesion treatment than partial treatment.
Conclusions: Total number of described vascular loop structures and their density or volume well reflected the existence, progression, and remission of soft-tissue AVMs. Topological analysis can be expected to be developed into a quantitative evaluation for AVMs. *(Plast Reconstr Surg Glob Open 2014;2:e207; doi: 10.1097/GOX.0000000000000151; Published online 4 September 2014.)*

Soft-tissue arteriovenous malformations (AVMs), which are the representative high-flow vascular malformations, cause various different types of vascular abnormalities and clinical symptoms, depending on their site and extent. It remains difficult to discern the degree of AVM progression quantitatively and to formulate treatment plans.

The nature of AVM pathology is the multiple occurrences of abnormal connections between arteries and veins. The authors predicted that the number of arteriovenous shunts is most directly related to the progression and improvement of the condition and used 2 mathematical concepts, namely topology and graph theory, to outline a technique for calculating the total number of described vascular loop

*From the Departments of *Plastic Surgery, †Diagnostic and Interventional Radiology, and ‡Pediatric Surgery, Osaka University Graduate School of Medicine, Osaka, Japan.*
Received for publication December 27, 2013; accepted June 10, 2014.
Copyright © 2014 The Authors. Published by Lippincott Williams & Wilkins on behalf of The American Society of Plastic Surgeons. PRS Global Open is a publication of the American Society of Plastic Surgeons. This is an open-access article distributed under the terms of the Creative Commons Attribution-NonCommercial-NoDerivatives 3.0 License, where it is permissible to download and share the work provided it is properly cited. The work cannot be changed in any way or used commercially.
DOI: 10.1097/GOX.0000000000000151

Copyright © 2014 The Authors. Published by Lippincott Williams & Wilkins on behalf of The American Society of Plastic Surgeons.
PRS Global Open is a publication of the American Society of Plastic Surgeons.

structures from 3-dimensional (3D) imaging data in a previous study about the mathematical concept of the topological analysis.[1]

With the objective of applying topological analysis to practice, this study aimed to verify whether the number of detected vascular loops in AVMs is more than that of normal vessels, whether the number increased without medical intervention, and whether treatment led to a decrease in the number of vascular loops in AVMs. It is anticipated that if these objectives can be fulfilled, determination of loop number by imaging could be developed into a reliable index for evaluating the degree of AVM progression and therapeutic effects.

PATIENTS AND METHODS

Patient Population

The study protocol was approved by the Institutional Review Board at Osaka University Hospital (Osaka, Japan), and written informed consent was obtained from all patients. A retrospective study was conducted on the results of computed tomography angiography (CTA) from AVM patients who were seen on an outpatient basis at the Department of Plastic Surgery, Osaka University Hospital between January 2010 and January 2013. A total of 19 cases (11 men and 8 women; mean age, 34.3 years; range, 8–71 years) were targeted because they met the prescribed imaging conditions and contracted no other metabolic or circulatory underlying disease.

AVM diagnosis was performed by confirming an obvious mass of vascular loops at the site of the patient's chief complaint using color Doppler ultrasound. When patients decided to accept treatment based on the results of certain CTA imaging, treatment was conducted within 2 months of this examination. If imaging was performed to determine therapeutic effects, it was performed at least 6 months after treatment and once color Doppler ultrasound findings had stabilized. Furthermore, when patients chose monitoring over time rather than treatment, imaging was performed only if symptoms related to Schobinger staging (Table 1) worsened.

As a reference, the early phase abdominal CTA results of 18 breast cancer cases (women; mean age, 52.7 years; range, 40–75 years), where the blood vessels were examined to prepare for reconstructive mammoplasty with deep inferior epigastric perforator flap, were targeted as control results to meet the same imaging conditions and examined within the same period as AVM patients. No patient had other metabolic or circulatory underlying disease, and 2 plastic surgeons (K.Y. and M.K.) confirmed that no anatomical abnormalities were found in the control data.

Table 1. Schobinger Classification of AVMs

Stage	Features
I	Cutaneous blush/warmth
II	Bruit, audible pulsations, expanding lesions
III	Pain, ulceration, bleeding, infection
IV	Cardiac failure

CTA Data Acquisition

A multisection helical CT scanner with 16 detector rows (GE Light Speed Ultra 16, General Electric, Milwaukee, Wisc.) was used for CTA.

In AVM cases, a bolus-tracking technique was used to synchronize the arrival of contrast in AVM with the initiation of the scan. To monitor the arrival of contrast material, axial scans were obtained at the level of proximal arteries near lesions. A contrast-enhanced scan was obtained using nonionic contrast medium (Iopamiron 300, Schering, Osaka, Japan, 300 mg iodine/ml) at a flow rate of 3 ml/s with a power injector followed by a 40-ml saline chaser. Scans were automatically triggered using monitoring software to identify a rise of 100 HU in the proximal vascular segment. The standard contrast dose was 2 ml/kg body weight, and in cases with large lesions, contrast medium volume was regulated as appropriate to contrast the entire lesion. The scan parameters were as follows: detector collimation, 0.625 mm; gantry rotation period, 0.5 second; tube voltage, 120 kV; and the tube current ranged from 150 to 440 mA according to automatic modulation depending on scanned part size.

Images were reconstructed to 16-bit grayscale 512×512 pixel images with a standardized protocol with the same section thickness (0.625 mm) and similar field of view (head and neck, 180–280 mm; trunk, 320–345 mm; extremity, 140–240 mm). When conducting multiple tests on the same patient, a particular effort was taken to maintain the same imaging conditions for each test.

In control cases, scan parameters were as follows: detector collimation, 0.625 mm; tube voltage, 120 kV; field of view, 320–345 mm; and the bolus-tracking technique using the nonionic contrast medium and automatic tube current modulation same as AVM cases was used.

Disclosure: *The authors have no financial interest to declare in relation to the content of this article. The Article Processing Charge was paid for by the authors.*

Copyright © 2014 The Authors. Published by Lippincott Williams & Wilkins on behalf of The American Society of Plastic Surgeons.
PRS Global Open is a publication of the American Society of Plastic Surgeons.

Vascular Lumen Identification

The DICOM image stacks acquired through imaging were processed using OxiriX version 5.5.2 (OxiriX foundation, Geneva, Switzerland) open source medical imaging processing software[2] on a regular MacOS X (Apple, Inc., Cupertino, CA) home computer.

At first, only the bony regions were eliminated using the bone removal function while confirming the volume rendering 3D images. Next, continuous regions rendered from CT values over 120 HU were considered contrast medium and extracted en masse by the region growing method and using the feeding artery origin as the starting point in AVM cases (Fig. 1A). By doing this, the vascular lumen of only the lesion area is rendered as a continuous, single area.

When using test results obtained at different times from the same patient, care was taken to use image stacks of the same number of slices with fixed points such as junctions of well-known blood vessels and feeding arteries as reference points so that the region of interest was maintained constant. In control cases, enhanced vessels from the level of renal artery to lateral circumflex femoral artery were cropped (Fig. 2)

Binarize

Thereafter, data were processed using ImageJ version 1.46 (National Institutes of Health, Bethesda, Md.) open source image processing software[3] and the BoneJ version 1.3.9 plug-in.[4] Rendered areas were binarized into monochrome images with the command "Make Binary," and the vascular lumen was converted into a 3D structure with clearly defined borders (Fig. 1B)

Purify

Next, topological noise was reduced by filling in the enclosed spaces in the 3D structure using the "Purify" command.[5] As no other soft tissue was suspended in the vascular lumen, these enclosed spaces signified thrombus or blood that did not contain any contrast medium. We calculated

$$\text{Vascular lumen capacity (ml)} = \frac{[BV]}{1000}$$

on the basis of [Bone Volume (BV)] (mm^3) calculated with the [Volume fraction] command.

Skeletonize

With the [Skeletonize 3D] command,[6] the thickness of all trabeculae in the 3D structure was converged into 1 voxel (volumetric pixel; Fig. 1C), and the 3D structure was simplified into a wire frame–shaped model while preserving data regarding vascular continuity.

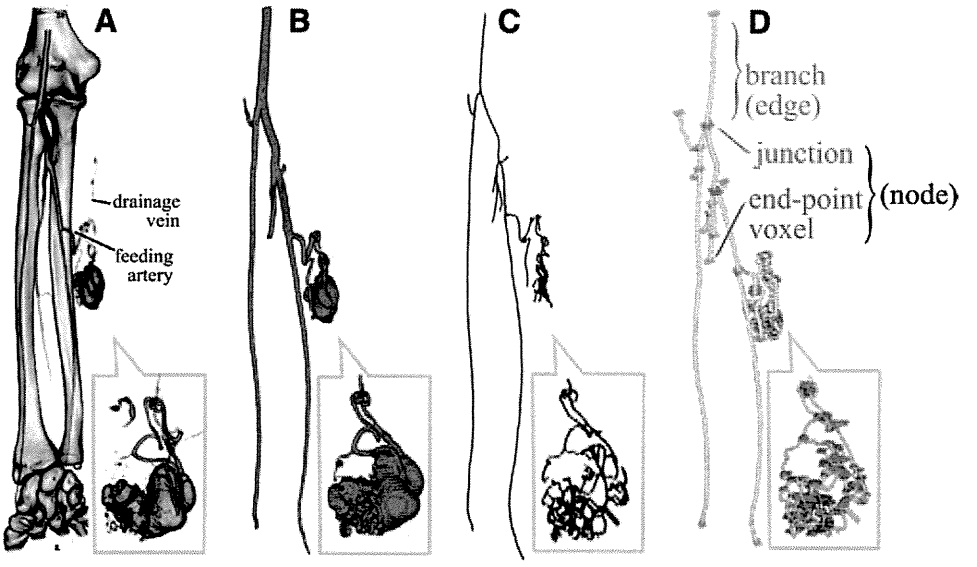

Fig. 1. Workflow images of topological analysis in a sample case (case 10: 15 years old, female, right forearm AVM). Gray squares indicate AVM lesion areas. A, Volume rendering 3D image of early phase CTA. Continuous regions rendered from CT values over 120 HU were extracted en masse by the region growing method and using the feeding artery origin as the starting point of the AVM lesion area. B, Rendered areas were binarized, the vascular lumen was converted into a 3D structure with clearly defined borders, and topological noise was reduced by filling in the enclosed spaces in the 3D structure. C, The thickness of all trabeculae in the structure was converged into 1 voxel (volumetric pixel). The vascular structure was simplified into a wire frame–shaped model while preserving its connectivity. D, The wire frame–shaped structure is considered as a graph, and the junction voxels/end-point voxels/branches are tagged and numbered.

Copyright © 2014 The Authors. Published by Lippincott Williams & Wilkins on behalf of The American Society of Plastic Surgeons.
PRS Global Open is a publication of the American Society of Plastic Surgeons.